AUTOMATING THE EXTRACTION OF REVOLUTION OBJECTS FROM SINGLE LASER SCANS OF ARCHITECTURAL SCENES

M. Deveau, G. Letellier, N. Paparoditis
Institut Geographique National, Laboratoire MATIS, 2, 4 avenue Pasteur 94165 Saint-Mandé Cedex
matthieu.deveau@ign.fr, guillaumeletellier@free.fr, nicolas.paparoditis@ign.fr

KEY WORDS: scanner laser, 3D Reconstruction, surface of revolution, profile estimation, range image

ABSTRACT

This paper focuses on the reconstruction of surfaces of revolution. We propose a method for estimating those surfaces from point clouds. We are more particularly dealing with data coming from one unique laser scanner acquisition; indeed, our approach extensively uses the range image topology. It makes originally use of geometric properties of surfaces of revolution. We firstly get an approximation of the axis of revolution, thanks to a Hough transform of symmetry axis computed on range image contours. Robust and accurate axis estimation refinement of position and orientation is then reached by minimizing the rms error of the profile estimate. Image topology is also used to estimate the object's profile. 3D points are connected following the image topology and the nearest neighbouring planes rotating around the axis of revolution. After projection on these planes, lines connecting points allow easy profile estimation. This method solves the measuring noise issue which is usually sorted out through moving least squares solutions. Once the object of revolution has been reconstructed, we retrieve automatically all occurrences of this pattern in the scene, with a scale adaptative matching algorithm.

1. GENERAL CONTEXT

The ARCHIPOLIS project, from the MATIS laboratory of the Institute G´eographique National (IGN), is dealing with high scale city model reconstruction. A general strategy is proposed combining aerial and terrestrial high resolution stereo imaging on streets and fac¸ades and dense laser and image acquisition on main cultural heritage buildings. Complementarity and continuity with aerial building reconstruction methods is also studied (Paparoditis et al., 2005).
In this framwork, detailed reconstruction of cultural heritage buildings from laser data and image is the scope of this paper. Architectural scenes reconstruction of great heritage value is especially important to reach a realistic representation. In this context, one goal is to get a compact structured surface representation, with a high geometric accuracy. We aim metrological applications for architects and surveyors, for restoration purpose and archiving.
As cultural heritage buildings have got more complex structures than apartments blocks, photogrammetry leads to long surveys, that much longer than architecture is complex. On the other side, laser scanners bring quickly a dense geometrical information on complex parts. In this context, we are studying a methodology using both laser data and image to ease segmentation and reconstruction (Deveau et al., 2005). In this article, we consider the segmentation part achieved and deal with the reconstruction part of/on one specific structure: the Surface Of Revolution (SOR), caracterized by its profile and its axis of revolution. In this article, which reports our first works on this field, only laser data are considered to achieve reconstruction while image is only used for texturing.

1.1 Related works

Many solutions for the reconstruction of SOR have been proposed and are still studied. Many of them deal with a single perspective view, either calibrated (Gr ¨un, 1975) (Wong et al., 2002) or uncalibrated (Utcke and Zisserman, 2003) (Colombo et al., 2005) and from silhouette's contours. (Neviata et al., 1995) have proposed methods of estimating generalized cylinders from multiple images. Other ways of looking for SOR reconstruction have followed the growth of range measuring systems (Pottmann et al., 2002) (Willis et al., 2001). These latter approaches have the drawback to lead to non-linear system minimization.

1.2 Data characterization

We make use of the range image and the intensity image, the latter coming from the backing laser intensity measure and belonging to the same image geometry as the range image (figure 1.2). Objects we are considering are usually scanned so that more than one thousand points lie on their surface. Intensity range is spread out on 8 bits. Standard deviation noise on distance is calibrated to 2 mm at 10 m (scanning conditions used for our experiments).

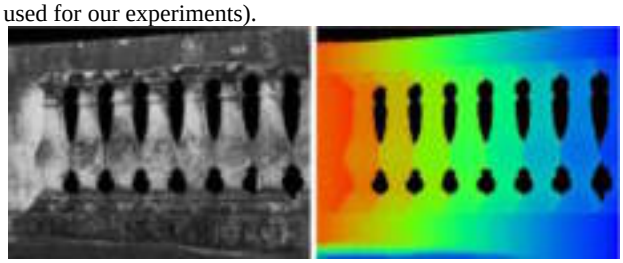

Figure 1: Range image and intensity image on a balustrade.

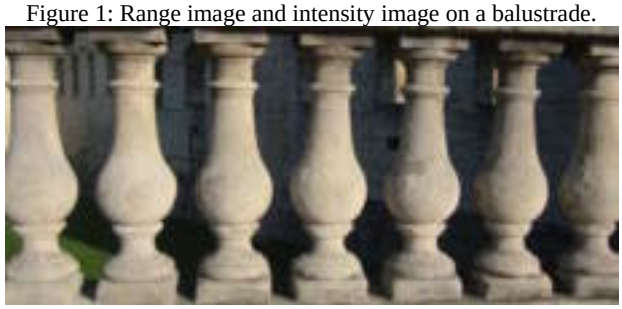

Figure 2: High resolution image.

2. EXTRACTING THE OBJECT SILHOUETTE

The SOR object is generally bounded by discontinuities which are well characterized both in the range image and in the intensity image. And because the SOR bounds symmetry around axis of revolution is kept in the range image, a first axis estimate can be solved.
We use a Hough transform on contour points coming from a

Canny-Deriche edge detection in the range image. Considering a couple of points $(M_i, M_j)=((x_i, y_i), (x_j, y_j))$from the contour chains, median axis parameters ρ and θ are the voting parameters :

$$\rho = \frac{|c|}{\sqrt{(x_j - x_i)^2 + (y_j - y_i)^2}} \qquad c = \frac{1}{2}\left(\|M_j\|^2 - \|M_i\|^2\right)$$

$$if\ \rho \neq 0\ \ \theta = \arctan\left(\frac{(y_j - y_i)\times c}{(x_j - x_i)\times c}\right)\ else\ \ \theta = \arctan\left(\frac{(y_j - y_i)}{(x_j - x_i)}\right)$$

Hough space sampling for this accumulation is set to one pixel for ρ and one degree for θ. From the 2D axis, we can get a 3D symmetry plane, where the axis of revolution should lie. Uncertainty of the 2D axis estimation can be computed: this defines a corresponding uncertainty on the 3D symmetry plane.

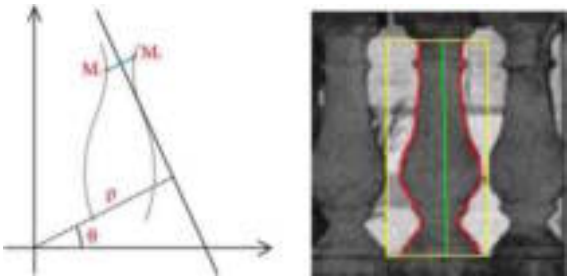

Figure 3: Symmetry axis detection from contours

Let us note that a first approximate of the axis of revolution could be achieved with the same algorithm, using two images from two different points of view, followed by the intersection of the two symmetry planes.

3. ESTIMATING THE 3D AXIS OF REVOLUTION

In this paragraph, we investigate axis of revolution estimate through a volumetric accumulation approach.

3.1 3D voting

This approach can be seen as an occupancy grid approach, with a discrete sampling of a workspace that encodes probability of occupancy at each grid point. The workspace is a box defined around the 3D plane according to uncertainty on the plane. Each voxel of the 3D grid stores the sum of the distances between the lines handled by the surface normals and the voxel. An intrinsic SOR propriety lies in the intersection of the lines handled by the normals on the axis of revolution. The 3D grid of voxels is defined around the 3D symmetry plane.
Normals are estimated on a quadratic surface computed on the k nearest neighbors, which allows to take into account point density variation and the discontinuity issue. The quadratic surface estimation is done in two paths: a first least square estimate followed by a rejection of outliers and a second least square estimate on inliers. The quadric surface normale gives an approximation of the normal on the point.
Let us consider a discretized volume, which consists of voxels V. S is a threshold corresponding to the radius of the voxel and $d_\perp$ the orthogonal distance between the voxel center and the line *Dn* handled by the normal and the 3D point. The distance function used for the voting step is as follow:

$$d(V, Dn) = \exp^{-2\frac{d_\perp(V,Dn)^2}{(s/2)^2}}$$

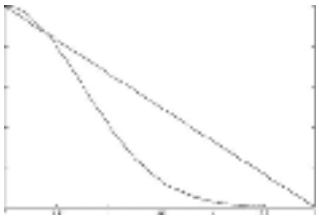

Figure 4: Distance function with S = 3 mm

The voxel score is then:

$$Score(V) = \sum_{n \in N} d(V, Dn)$$

Figure 5: 2D cut of the voting geometry. Distances between lines (red) handled by the normales (black) and the voxel centers (green) are summed

After the voting step, a first estimate of the axis is given through weighted least squares, after a filtering stage on robust inertia axis estimate. The weight corresponds to the voting score.

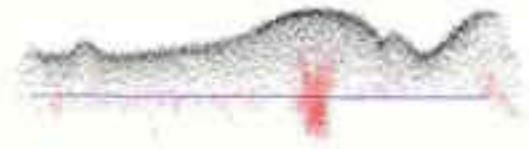

Figure 6: Point cloud (black) and approximated axis (blue) on filtered points (red, 824 points upon 16496 marked voxels)

3.2 3D revolution axis estimation improvement

A significative improvement of the axis estimation can be achieved with a local search near the first estimate. A good criterion should be defined to assess the axis quality. The first solution studied consists in computing the rms error on the 2D profile. Estimating the aspect ratio of points projected onto a plane orthogonal to the revolution axis tested would be a better solution: there is no need to compute the profile for each estimate. The aspect ratio corresponds to the ratio between the radius of the minimum including circle and the radius of the maximum included circle. This leads to a quicker estimate, and leaves independant the axis estimate and the profile estimate.

4. RECONSTRUCTING THE OBJECT'S PROFILE

We can now get a 2D point cloud by 3D points projection on the plane rotating around the revolution axis. The projection plane is defined by the axis of revolution and the point to project 7.

Figure 7: 3D point cloud after plane sweep projection around the axis of revolution

4.1 Reducing noise with the Mobile Least Squares method

Making the assumption that measuring noise follows a Gaussian distribution, this noise can be smoothed by the moving least squares method (Lee, 2000). This method comprises four steps: scrolling through the 2D point cloud, defining a local tangential frame, estimating a quadratic form, and projecting points onto the quadratic form.
Mobile least squares corresponds to the local use of weighted least squares. Mobile least squares allow to thin the point cloud without smoothing too strongly the signal. A quadratic form is estimated locally on a neighbourhood, minimizing the expression:

$$\sum_{i \in N} \left(a x_i^2 + b x_i + c - y_i \right)^2 w_i$$

where each w_i is a weight regarding to distance.
This minimization is solved by the classical weighted least squares formulation:

$$W_{n,n} A_{n,m} X_{m,1} = W_{n,n} B_{n,1}$$

Matrix A and B are balanced with a square matrix W where the diagonal terms store weights. The solution will be:

$$X = (A^t W^t W A)^{-1} A^t W^t W B = (A^t W^2 A)^{-1} A^t W^2 B$$

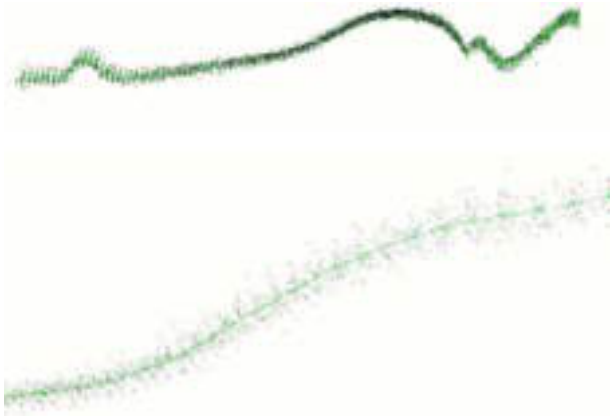

Figure 8: Thined point cloud, complete object and detail

4.2 Final profile reconstruction

The thining step is followed by a sampling one, achieved by median points estimate, to reduce the amount of data. Discontinuity points should be introduced to constrain the curve.

Figure 9: Results on median points sampling

Once noise on the cloud has been reduced, the profile is represented with a cubic spline (figure 10).

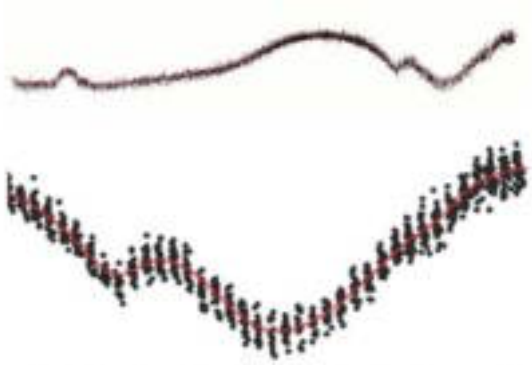

Figure 10: Point cloud and spline (red), entire object and detail

5. EVALUATION

Real data have been digitized with various resolutions. We can first note that RMS error is lower than theorical standard deviation (2 mm). But if finer resolution gives better results, it implies longer acquisition field work and also longer post-processing.

Scan resolution	points number	RMS (mm)
0.28 mrad – 2.8 mm at 10 m	27241	1.4
0.36 mrad – 3.6 mm at 10 m	8643	1.9
0.84 mrad – 8.4 mm at 10 m	2053	2.1
1.1 mrad – 11.2 mm at 10 m	1388	2.3

Table 1: RMS error for different scan resolutions

Visualizing spatial repartition of error shows that the axis of revolution and the profile are both well centered: random distribution of error corresponds to measuring noise and surface roughness.

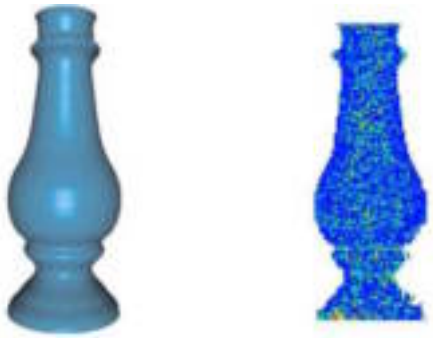

Figure 11: 3D model and error image for a balustrade feature. Error scale: 0-2.5 mm in blue, 2.5-5 mm in green, 5-8 mm in red

6. MULTIPLE MODELS INFERENCE DETECTION BY SCALE ADAPTIVE TEMPLATE MATCHING

Getting each inference of the same object in the scene is done by range template matching pararo1998. Normalized cross-correlation between a reference range image of the object and the entire range image returns a score map, where maxima gives the inferences positions. This is true under constant scale hypothesis. Scale adaptive matching will allow to recover every inferences. Since correlation must be done only on the object, a binary mask is used to consider only corresponding shape.

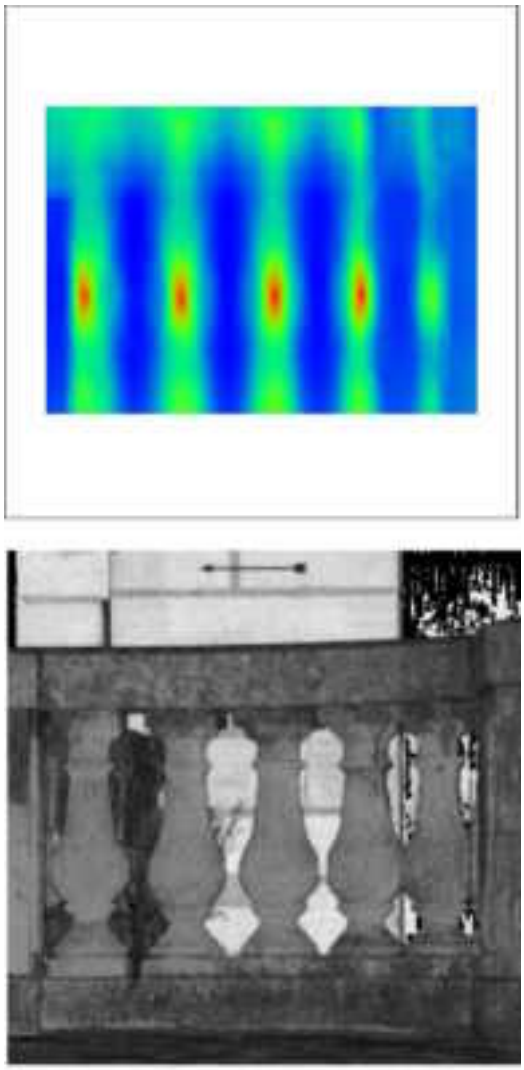

Figure 12: Correlation scores

7. CONCLUSION AND PERSPECTIVES

We have proposed an approach using range image geometry to estimate a surface of revolution, through its axis and profile recovery. Using the symmetry on the shape contours allows to restrict search space and so on, to reduce computation time. Despite this point, this is a first attempt, and it should be improved for a few reasons: first, quality criterion for the axis estimate should be independant from the profile estimate. Second, multi-resolution shame could accelerate the axis finer estimate. Then, discontinuity detection in the profile should be added. We may also study the effect of fusing multiple viewpoints: getting points on the whole surface should improve axis detection, while reducing the search space. Finally, pattern recognition in the profile may simplify the object description, using procedural grammars built upon architectural knowledge (Dekeyser et al., 2003).

REFERENCES

Colombo, C. and del Bimbo, A. and Pernici, F., Metric 3D Reconstruction and Texture Acquisition of Surfaces of Revolution from a Single Uncalibrated View, PAMI, Vol. XXVII, pp. 99-114, 2005.

Dekeyser F., Gaspard F., De Luca L., Florenzano M., Chen X., Leray P., Cultural heritage recording with laser Scanning, computer vision and exploitation of Architectural rules, in Proc. of International Workshop on vision techniques for digital architectural and archaeological archives -Ancona, 2003.

Deveau M., Paparoditis N., Pierrot-Deseilligny M., Chen X., Thibault G., Strategy for the extraction of 3D architectural objects from laser and image data acquired from the same viewpoint, in Proc. 3D-ARCH ISPRS Workshop, 2005.

Dey T. K., Kumar P., A simple provable algorithm for curve reconstruction, in Proc. 10th. ACM-SIAM Symposium on Discrete Algorithms, 1999.

Dey T. K., Wenger R.,Reconstructing curves with sharp corners. Computational Geometry Theory Applications, vol 19, 2001.

Gruen A., Photogrammetric reconstruction of rotation surfaces from single photographs. In German. Deutsche Geodtische Kommission, Reihe C, No. 212, Mnchen 1975.

Lee I.-K. Curve reconstruction from unorganized points. Computer Aided Geometric Design 17(2), pp. 161-177, 2000.

Paparoditis N., Cord M., Jordan M., Cocquerez J.P., Building detection and reconstruction from mid-and high-resolution aerial imagery, Computer Vision and Image Understanding, Volume 72 , Issue 2, pp. 122 -142, Nov. 1998.

Paparoditis N., Bentrah O., Penard L., Tournaire O., Soheilian B., Deveau M., Automatic 3D Recording and Modeling of Large Scale Cities: the ARCHIPOLIS Project, in Proc. of Recording, Modeling and Visualization of Cultural Heritage Conference, Ascona, May 2005.

Pottmann H., Leopoldseder S., Wallner J., Peternell M., Recognition and reconstruction of special surfaces from point clouds, Archives of The Photogrammetry, Remote sensing and Spatial Information Sciences, 2002.

Ulupinar, F., and Nevatia, R., Shape From Contour: Straight Homogeneous Generalized Cylinders and Constant Cross-Section Generalized Cylinders, PAMI(17), No. 2, pp. 120-135, 1995.

Utcke S. and Zisserman A., Projective reconstruction of surfaces of revolution, in Proc. DAGM-Symposium Mustererkennung, pp. 265-272, 2003.

Willis A., Orriols X., Velipasalar S., Cooper D. B., Binefa X., Extracting Axially Symmetric Geometry From Limited 3D Range Data, SHAPE Lab Technical Report, 2001.

Wong K.Y.K., Mendona, P.R.S., Cipolla, R., Reconstruction of surfaces of revolution from single uncalibrated views, in Proc. Brit Mach Vision Conf, 2002.

Zhang Z., Parameter Estimation Techniques: A Tutorial with application to Conic Fitting, Image Vision Computing 15, 1997.